ELSEVIER

Journal of Nuclear Materials 290–293 (2001) 173–179

journal of nuclear materials

www.elsevier.nl/locate/jnucmat

Chemical erosion of doped graphites for fusion devices

C. García-Rosales [a,*], M. Balden [b]

[a] *Centro de Estudios e Investigaciones Técnicas de Gipuzkoa and Escuela Superior de Ingenieros, Universidad de Navarra, P.O.B. 1555, 20009 San Sebastián, Spain*

[b] *Max-Planck-Institut für Plasmaphysik, EURATOM Association, Boltzmannstr. 2, D-85748 Garching, Germany*

Abstract

Doping of carbon generally results in a reduction of its chemical reactivity during hydrogen ion bombardment. Due to preferential sputtering of carbon, the dopants may be enriched at the surface, resulting in an additional reduction of the erosion yield. Dopants in the form of sub-μm precipitates with a very homogeneous distribution lead to in a more effective reduction of both chemical erosion processes, Y_{therm} and Y_{surf}. However, dopants may degrade the thermal conductivity of graphite, which has to be avoided. First results on the development of carbon materials doped with different carbides and with optimized microstructure and thermomechanical properties show that VC acts as an effective catalyst for graphitization causing an improvement of the thermal conductivity. It leads further to a reduction of both, the Y_{therm} and the Y_{surf} chemical erosion processes, which is partly attributed to surface enrichment but is also the result of a chemical influence.

Keywords: Chemical erosion; Doped carbon; Carbide; Graphite; Thermal conductivity

1. Introduction

The use of graphite or carbon fiber composite (CFC) materials for those areas of the vessel walls receiving the highest plasma loads, i.e. at limiters and divertor plates, appears to be indispensable for operation in future fusion devices such as ITER [1] due to their unequalled thermomechanical properties. A critical point is its relatively large erosion during hydrogen bombardment from the fusion plasma. In addition to physical sputtering, carbon shows enhanced erosion by chemical sputtering, i.e. the formation and release of hydrocarbons (see e.g. [2–5]). This represents a limitation on component lifetime, and leads to plasma dilution with impurities. Besides, the enhanced erosion is correlated with the production of co-deposited layers, representing a major concern in view of the high tritium inventory trapped in these layers [6]. Possible alternatives to this concern regarding the material choice would be:

- To restrict the use of carbon materials to the few surface areas receiving extreme heat loads.
- To develop improved carbon-based materials with reduced chemical erosion, optimized thermomechanical properties, and with reduced hydrogen retention.

In the last decades several investigations have been performed on the effect of dopants, i.e. of small additions (several at.%) of other elements to carbon, on the chemical erosion [7–23] and on the hydrogen retention [8,15,24–27]. Recent investigations [22] suggest that, besides the dopant elements, also microstructure effects, such as dopant distribution, dopant particle size and porosity, play also a very critical role.

On the other hand, the thermal conductivity and the large thermal shock resistance of carbon-based materials should not be degraded but rather be improved by doping. It is known that some metals and carbides act as catalyst for the graphitization of amorphous carbon [28–30] resulting in a higher thermal conductivity. This holds for dopants with no or very little solubility in the graphite lattice. However, if they are soluble in the graphite lattice, as in the case of B [31], their beneficial effect as catalyst for graphitization is offset by the loss of thermal conductivity due to increased phonon scattering [32].

* Corresponding author. Tel.: +34-943 21 28 00; fax: +34-943 21 30 76.

E-mail address: cgrosales@ceit.es (C. García-Rosales).

0022-3115/01/$ - see front matter
PII: S0022-3115(00)00567-5

This means that the manufacturing procedure of doped carbon materials as well as the choice of the proper dopant elements or compounds and their grain sizes play an essential role for obtaining a carbon-based material with optimized properties. Up to now mostly commercially available materials have been investigated with respect to their use as plasma facing materials. They had been optimized for other purposes, such as the space program. Optimization of carbon based materials for plasma-facing areas in view of a reduction of all process of chemical erosion, while improving their thermal conductivity and mechanical properties, seems possible and necessary. This task requires a deeper understanding of the reduction mechanisms of chemical erosion of carbon materials by doping, together with a further development of the manufacturing procedure.

In this paper it is tried to review today's understanding of the mechanisms of chemical erosion of carbon by hydrogen bombardment and to describe the influence of doping on chemical erosion. The relevance of microstructure effects in view of a reduction of chemical erosion will be shown. Finally, first results on the development of isotropic graphite doped with different carbides and their response concerning chemical erosion are presented.

2. Mechanisms of chemical erosion

The mechanisms governing the chemical erosion of carbon under hydrogen bombardment have been summarized in recent reviews [2–5,33,34].

Two processes contribute to the chemical erosion of carbon under hydrogen bombardment:

(1) A *thermal activated process*, with an erosion yield Y_{therm}. The incident hydrogen atoms are slowed down in the surface layer of the solid. They interact with sp^2 carbon atoms at the edges of graphitic planes or with broken bonds producing sp^3 CH_3 complexes. These CH_3 radicals may be released already at temperatures above 400 K while returning to the basic sp^2 configuration. With further increasing temperature, the incoming hydrogen may recombine with adsorbed atoms, thus interrupting the hydrogenation process. Hence, the thermally activated chemical erosion yield exhibits a pronounced maximum between 600 and 900 K, depending on the experimental parameters. The reaction steps of this thermal activated process were first elucidated by Küppers et al. [33,34]. An analytical expression for this erosion process based on these reaction steps was first provided by Roth and García-Rosales [3] and improved by Mech et al. [4] and Roth [5]. No dependence on the hydrogen isotope is observed for this process.

This thermal activated process is enhanced by radiation damage, which is produced by kinetic energy transfer from incident ions to lattice atoms, providing active sites for the reaction with incoming hydrogen and thus increasing chemical erosion. Due to the kinetic nature of this process, Y_{therm} depends also on the hydrogen isotope in the energy range above a threshold energy for damage production [3–5].

(2) A *surface process*, which is described by Y_{surf}. At low incident ion energies (<100 eV) the formation of sp^3 hydrocarbon complexes, i.e. hydrogenation occurs only at the surface. The CH_3 radicals have a low surface binding energy (about 2 eV compared to 7.4 eV for C atoms on the bulk) and may be ejected kinetically by incident hydrogen atoms. Thus, this process can be described in a similar way as physical sputtering, with a threshold energy in the low eV range.

For the application of carbon as divertor material, the process described by Y_{surf}, resulting in a reduction of the threshold energy for sputtering, is very critical. On the other hand, the changes in thickness over the life of divertor plates in future fusion devices will result in a variation in surface temperature over a wide range, which will affect Y_{therm}. Therefore, it is important to find ways to reduce *all* processes of chemical erosion without detriment of other important properties for divertor application such as the thermal conductivity and the mechanical strength.

3. Influence of dopants on chemical erosion

Up to the middle of the 1990s most of the investigations about the reduction of chemical erosion by doping were concentrated on B-doped graphites [2,7–16,22,23]. However, in the last years the effort was extended to Si- [7,10,12,16–18,20,22,23,35,36,43,44] and Ti-doped graphites [9,10,15–18,22], as well as on multi-element [19,21] and W-doped graphites [16]. Some limited work was done on Fe-, Cr- [14] and V-doped graphites [9]. These experiments were performed for a wide range of incident energies and fluxes, and with different experimental methods (mass spectrometry, weight loss). Besides, the concentration and chemical state of the dopants as well as the quality and microstructure of the materials were mostly very different and not well known. This represents a problem in comparing the available data. Nevertheless, a systematic regarding the influence of different dopants on Y_{therm} and Y_{surf} can be pointed out. In the following, the relevant trends will be reviewed.

3.1. Influence of doping on Y_{therm}

Isotropic graphite with boron addition above 3 at.% shows a large reduction in the thermal chemical erosion, Y_{therm} [7–14], likely due to the change in the electronic structure of neighboring carbon atoms by substitutional

boron. The effect of boron doping on the chemical bonding of graphite was investigated by Küppers and co-workers [37] for thin a-C/B:H films. They came to the conclusion that boron doping leads to an enhanced H content as compared to undoped films, hence the average bonding strength of hydrogen and methyl groups to the film networks decreases. This behavior is supported by the finding that the thermal desorption of H_2 from boron-doped graphite implanted with hydrogen ions occurs at temperatures about 150 K lower than for undoped graphite [15,26]. It can be concluded that boron doping enhances the recombinative release of hydrogen in the form of H_2, resulting in a reduced thermal erosion yield and a shift of the temperature of the maximum yield to lower temperatures. Indeed, the experimental results for the temperature dependence of the chemical yield of boron-doped graphite USB15 (15 at.% B) at different energies could be fitted with the above analytical model by assuming a reduced activation energy for hydrogen release with all other parameters unchanged [5].

For other dopants such as Si, Ti, V and W a reduction of the thermal activated process, Y_{therm}, of at least a factor of 2 compared to pure graphite has been found [9,16,17]. This is shown in Fig. 1(a) for a Si- and a Ti-doped graphite, in comparison with pure and B-doped graphite. Here the methane formation yield is plotted as a function of the target temperature for 1 keV D^+ bombardment. The reason for this reduction is not yet well understood. These dopants do not exhibit any solubility in graphite, which would explain an influence on the electronic structure of neighboring carbon atoms, as for the case of B.

Furthermore, the temperature of the hydrogen desorption shows in the case of Si and W doping only an insignificant shift with respect to pure graphite [25,26].

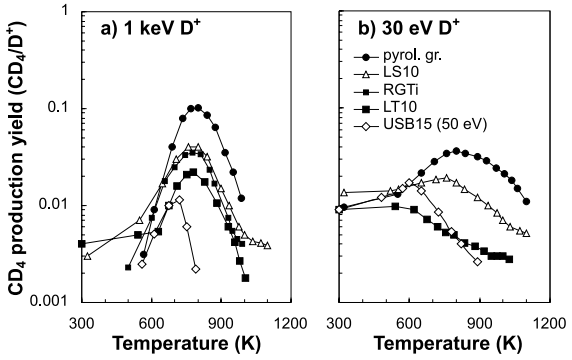

Fig. 1. Temperature dependence of the methane formation yield of pyrolytic graphite [13], and the doped graphites LS10 (10 at.% Si) [17], LT10 (10 at.% Ti) [17], RGTi (2 at.% Ti) [15] and USB15 (15 at.% B) [13] for (a) 1 keV and (b) 30 eV D^+ bombardment.

In the case of Ti doping, however, a two-peak structure is observed in the temperature dependence of the hydrogen desorption. The low temperature peak (~600 K) corresponds to the hydrogen release from TiC while the high temperature peak arises at about the same temperature as pure graphite [15,25,26]. Consequently, for doping with Si and W a much smaller reduction of the thermal chemical erosion is observed compared to B doping [16,17], whereas for Ti doping the reduction observed is the larger the higher is the Ti concentration and thus the amount of TiC present in the sample [15–17]. This is shown in Fig. 1(a), where two Ti-doped graphites with 2 at.% Ti (RGTi) and 10 at.% Ti (LT10), respectively, are compared. The erosion data of the Si-, Ti- and W-doped graphites measured by Chen et al. [16] have been fitted by Roth [5] with the model described above, coming to a small reduction of the activation energy for hydrogen release compared to pure graphite, but not as strong as for B-doped graphite.

Changes in Y_{therm} may also be caused by a surface enrichment of the dopants. A metal enrichment to about 25 at.% at the surface would already explain a reduction of the erosion yield by a factor of 2 [22]. For B doping, no significant enrichment has been observed for ion energies and temperatures in the range of Y_{therm} [38]. In contrast, for Si- and Ti-doped graphite a carbidic enrichment for the parameter range corresponding to the thermal activated process is observed [39]. For TiC and SiC [39–41], as well as for B_4C [10], the hydrocarbon production is negligible. Even though, the observed carbidic enrichment does not explain all of the Y_{therm} reduction measured. The reason for the observed reduction of Y_{therm} for dopants other than B is likely a process influencing the chemical bonding of C. Therefore, a very fine and homogeneous distribution of the dopants in the graphite matrix should result in a more effective reduction of Y_{therm}. Hence, dopants in the form of small precipitates (sub-micron or nanometer range) are expected to exhibit lower erosion yields.

3.2. Influence of doping on Y_{surf}

The surface chemical erosion process dominates at low incident energies and low surface temperatures. Other than for Y_{therm}, boron addition to graphite does not lead to a noticeable reduction of Y_{surf} [13], indicating that the hydrogenation of carbon atoms at low temperatures is not influenced by boron. For other dopants such as Si and Ti, the subthreshold erosion at temperatures below 600 K is also almost unchanged. This is shown in Fig. 1(b), where the methane formation yields for pure graphite and Si-, Ti- and B-doped graphite are plotted as a function of target temperature for 30 eV D^+ bombardment.

Because carbon is eroded preferentially by hydrocarbon release, a dopant enrichment at the surface must

be expected until a steady state is reached, where the composition of the sputtered particles is equal to the bulk composition [42]. Therefore, at high fluences a reduction of the carbon erosion is expected. This effect should be the more pronounced the higher the threshold energy for physical sputtering of the dopant atoms. Hence, dopants with higher atomic mass will be more advantageous. Indeed, dopant enrichment has been observed for Si- and Ti-doped graphite, as can be seen in Fig. 2, where the fluence dependence of the Si and Ti surface concentration for a Si- and a Ti-doped graphite is shown. As a consequence of the surface enrichment owing to preferential sputtering of C, a surface topography with a columnar structure develops, where carbidic grains protect the underlying graphite from further erosion [22]. This change in surface composition up to a steady-state results in a decrease of the total erosion yield at high fluences, as observed experimentally for a Ti-doped graphite at 20 eV D^+ bombardment, i.e. below the threshold for physical sputtering of Ti. For Si-doped graphite, however, no drastic reduction with fluence at 20 eV could be observed. This may be caused by the low threshold energy for physical sputtering of SiC of the order of 10 eV [39], or most probably due to either chemical erosion of Si in form of silane molecules or to chemical erosion of C from SiC, as reported in [40].

A steady-state surface topography with reduced chemical erosion will be reached when a surface layer of a thickness larger than about the mean dopant particle distance is eroded [17,22]. The time to reach this steady-state surface topography will be the shorter, and the thickness of the modified surface layer the thinner, the more homogeneous is the distribution of dopants in the carbon matrix and the smaller is their particle size. This is very important in view of off-normal events taking place in tokamaks such as disruptions and ELMs, where this topography may be destroyed by sublimation or brittle fracture. For a doped graphite with a dopant particle size of a view μm and a meal particle distance of several μm, exposed to a flux as expected in the divertor of future fusion devices (10^{23}–10^{24} D/m^2 s), the time to reach this steady state surface composition is of the order of 10–100 s [22].

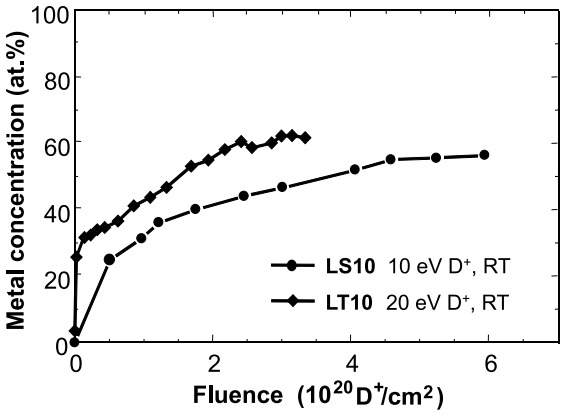

Fig. 2. Fluence dependence of the Si or Ti surface concentration during low energy D^+ bombardment for the 10 at.% Si-doped graphite LS10 and the 10 at.% Ti-doped graphite LT10 [39].

4. Development of doped carbon materials

From the results reported it can be concluded that the keys for developing improved doped-carbon materials are the proper selection of dopants as well as the improvement of the microstructure. Dopants should have a double function:

1. To reduce efficiently both processes of chemical erosion (Y_{therm}, Y_{surf}) and, as far as possible, the hydrogen retention.
2. To act as catalyst for graphitization in order to obtain a carbon material with improved thermal conductivity. However, they should exhibit no or very little solubility in the graphite lattice in order to avoid the loss of thermal conductivity of the graphite.

The first point requires the development of a graphite material with a very homogeneous distribution of dopants in the matrix and with low porosity, in which dopants have a particle size a small as possible. The scored point demands a manufacturing procedure in which the dopants are mixed with the starting carbonaceous powder before graphitization.

To obtain such materials, investigations and development in a wide parameter range are needed. In the following, the first results on the development of doped isotropic graphite are briefly presented. These results are described in more detail in [43,44].

4.1. Manufacturing procedure and characterization

The development of doped carbon materials with improved plasma-surface-interaction properties has been started at the Materials Department of CEIT (Spain) in collaboration with the IPP Garching (Germany). This project includes the investigation and optimization of a wide range of manufacturing parameters. As starting material different types of self-sintering powders of microspheres of carbonaceous mesophases (MMC) based on petroleum residues are used. This MMC powder is an excellent starting material for the production of isotropic, extremely fine-grained binderless carbon, representing a novel path for the production of isotropic graphite with significantly improved strength [45,46].

The fabrication procedure followed in this work can be summarized as follows:

Table 1
Physical properties of the carbides selected as dopants [47,48]

Carbide	Melting point (°C)	Vapor pressure at 2000 K (bar)	Particle size (μm)	Thermal conductivity at RT (W/mK)
α-SiC	2.540	2.7×10^{-6}	~1	~150
TiC	3.150	7.6×10^{-10}	~1	30
V_8C_7	2.850	9.4×10^{-9}	1.5–2	30
ZrC	3.500	3.0×10^{-11}	~1	29
WC	2.870	4.0×10^{-11}	<5	100

- Jet-milling of the MMC powder to appropriate particle size distribution (<5 μm).
- Mixing and uniaxial molding (pressure 150 MPa) at 16 mm sample diameter and ~5 mm thickness.
- Sintering up to 1000°C in a nitrogen atmosphere. The mass loss is of the order of 13.5%.
- Graphitization up to 2100°C in an inert atmosphere.

As dopants, the following carbides have been selected up to now: α-SiC, TiC, V_8C_7, ZrC, WC. All these carbides except SiC are known to show a catalytic effect on graphitization [28,29]. As can be seen in Table 1, they exhibit a high melting point and a relatively low vapor pressure. The particle size of the carbide powders was in the range 1–2 μm (see Table 1) except for WC (<5 μm). The carbides were selected so that the metals cover a wide range in atomic mass. They were added to the carbon powder up to a metal concentration of about 5 at.%. For the case of TiC, a series ranging from 0.7% to 5 at.% was prepared to see the influence of the dopant concentration on chemical erosion. The graphitization temperature of this series was 2025°C.

Concerning the structural characterization of the samples, a wide program has been started and is in progress. [44].

After sintering at 1000°C the carbon material shows a turbostratic structure with very low crystalline order. During graphitization the unordered stacked carbon layer planes becomes more crystalline towards the perfect graphite structure while the crystallite size increases [49]. The crystallite height L_c can be easily determined from X-ray diffraction. Hence, the value of L_c is generally used for the determination of the degree of graphitization.

The value of L_c after graphitization is shown in Fig. 3 for samples with different dopants but the same at.% metal concentration (Fig. 3(a)), and with Ti as dopant at different concentrations (Fig. 3(b)). All carbides except SiC lead to an increase in L_c as compared with the L_c value of graphite without carbides. V_8C_7 shows the largest catalytic effect of all investigated carbides. For comparison, the L_c values of a commercial graphite (POCO) and of the 2 at.% Ti doped graphite RG–Ti (Efremov Institute, St. Petersburg [50]), are also shown. The RG–Ti material, which shows an extremely high thermal conductivity in one direction [50,51], exhibits also a high L_c value, indicating a high degree of crystallinity. The POCO material, on the other hand, shows about the same crystallinity as our graphite without dopants. Fig. 3(b) shows that the catalytic effect of TiC seems to saturate at about 3–4 at.% Ti.

The bulk density of the undoped specimen was determined geometrically in various stages of the graphitization treatment. It increases almost linearly from 1.61 g/cm^3 after sintering to a value of 1.92 g/cm^3, which is reached at 1700°C and remain nearly constant up to 2100°C. The theoretical density and the open porosity were measured pycnometrically.

In Fig. 4 the open and closed porosity is shown for pure graphite (MMC) and for graphite doped with different carbides in the same at.% metal concentration after sintering (1000°C) and after graphitization (2100°C). While pure carbon experiences a reduction of the total porosity of about 33% during graphitization, the reduction observed for graphite doped with SiC and VC, and in a lower extent for ZrC, is surprisingly small.

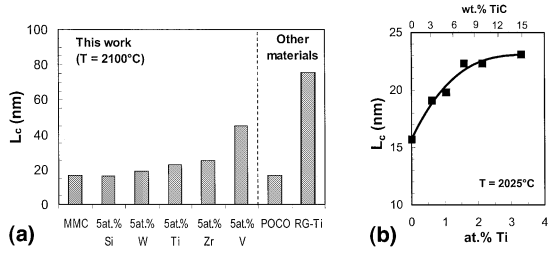

Fig. 3. Mean crystallite height L_c: (a) for samples with different dopants in the same at.% metal concentration graphitized at 2100°C, and (b) for Ti-doped samples graphitized at 2025°C as a function of the Ti concentrations. In (a) the L_c values for the commercial fine grain graphite POCO and for the Ti-doped graphite RG–Ti 91 are also shown.

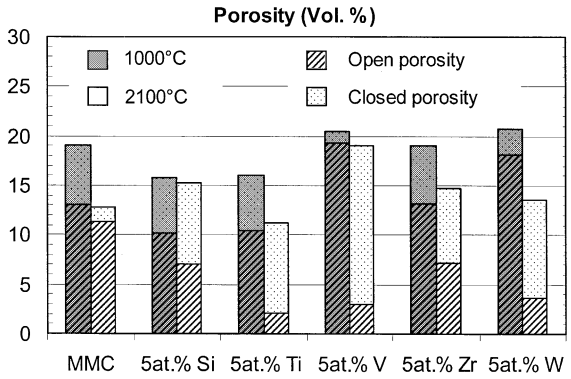

Fig. 4. Open and closed porosity after sintering (1000°C) and after graphitization (2100°C) for the manufactured specimens: pure graphite (MMC) and graphite doped with different carbides.

Furthermore, in the pure carbon sample most of the closed porosity vanishes during the graphitization process while the open porosity decreases slightly. In contrast, in all doped graphites the open porosity decreases significantly while the closed porosity becomes even larger than before graphitization. This effect is especially pronounced for the VC-doped graphite. This carbide shows, on the other hand, the highest catalytic effect on graphitization. In [29] the dissolution of unordered carbon in a metal carbide particle followed by the precipitation as ordered graphite is proposed as possible mechanism for the catalytic graphitization. As reported in [52], V_8C_7 experiences an order–disorder transition at a temperature of 1360–1380 K, i.e. just at the beginning of the graphitization process. In a disordered phase the amount of vacancies and thus the carbon diffusion should increase, which would explain the larger catalytic effect of this carbide.

4.2. First results on chemical erosion

The erosion experiments were performed at the Garching high current ion source [53]. First measurements of the erosion yields for 30 eV D impact at room temperature and accompanying measurements of the metal surface concentration (ion beam analysis, scanning electron microscopy) were performed [43].

Fig. 5 shows the erosion yield of the undoped, the W- and V-doped graphite versus the ion fluence. At the highest accumulated fluences, a reduction of the erosion yield by about 50% of the undoped material is found. However, the carbidic enrichment – responsible for the columnar topography on the eroded surface – results in metal concentrations of about 13 at.% W and 11 at.% V, corresponding to a surface area covered with carbide grains of less than 30%. This means that the geometrical shielding due to the carbide enrichment at the surface can only be responsible for about half of the observed yield reduction. It follows that the influence of these dopants on the surface process Y_{surf} is partly of a chemical nature and not only due to a surface enrichment by preferential sputtering.

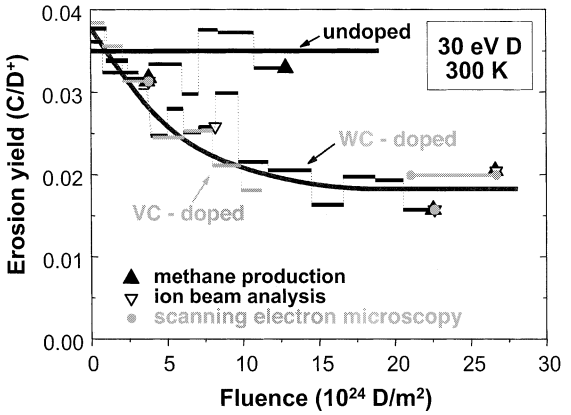

Fig. 5. Fluence dependence of the erosion yield for 30 eV D impact at room temperature for the undoped, the W- and the V-doped graphites (lines). The dots mark the fluences at which a temperature dependence for 1 keV D impact (▲) and the surface composition (ion beam analysis (▽), scanning electron microscopy (●)) were measured.

In addition, the temperature dependence of the CD_4 production yield was measured at the fluences marked with dots in Fig. 5 for 1 keV D^+ impact, in order to check the influence of dopants on Y_{therm}. In this case a reduction of the CD_4 production yield to below 50% of that of undoped graphite is observed. Again, from the knowledge of the dopant enrichment at the surface, it results that the addition of dopants leads to a reduction of the thermal process Y_{therm} that cannot be attributed alone to surface enrichment.

5. Summary

According to today's understanding, there are two processes contributing to chemical erosion of carbon by hydrogen impact:

- a thermal activated process, Y_{therm}, with a maximum of the erosion at 700–950 K, which dominates at incident energies in the keV range. This process is enhanced by radiation damage,
- a surface process, Y_{surf}, due to the kinetic ejection of hydrocarbon complexes formed in the very surface layers. This process dominates at low incident energies and low target temperatures.

Doping of graphite leads generally to a reduction of both chemical erosion process. The reduction of Y_{therm} seems to be partially due to a lowering of the activation energy for hydrogen release, even though dopant enrichment may also contribute to a part of this reduction. The reduction of the surface process, Y_{surf}, is mainly caused by dopant enrichment at the surface at high fluences owing to preferential carbon sputtering. For both processes, dopants in the form of sub-μm precipitates with a very homogeneous distribution would lead to a more effective reduction.

The addition of dopants should not degrade the good thermomechanical properties of graphite. Taking into account the catalytic effect of some metals and carbides on the graphitization, the potential for a development of improved doped carbon materials with reduced chemical erosion and optimized thermomechanical properties becomes evident.

First results on the development of new doped carbon materials show that VC acts as the most effective

catalyst for graphitization of all investigated dopants. It leads further to a reduction of both the Y_{therm} and the Y_{surf} processes, which is only partly attributed to surface enrichment but is also the result of a chemical influence in both cases.

Acknowledgements

We would like to thank the company REPSOL for providing the mesophase carbon powder for the manufacturing of the samples, as well as T. Gómez-Acebo for its kind assistance by using the Thermo-Calc software for the calculation of the carbide vapor pressures. Furthermore, the authors sincerely appreciate helpful discussions with R. Behrisch and J. Etxeberria during the preparation of the manuscript.

References

[1] ITER Physics Basis, Nucl. Fus. 39 (12) (1999).
[2] E. Vietzke, A.A. Haasz, in: W.O. Hofer, J. Roth (Eds.), Physical Processes of the Interaction of Fusion Plasmas with Solids, Academic Press, San Diego, 1996, p. 135.
[3] J. Roth, C. García-Rosales, Nucl. Fus. 36 (1996) 1647 with corrigendum Nucl. Fus. 37 (1997) 897.
[4] B.V. Mech, A.A. Haasz, J.W. Davis, J. Appl. Phys. 84 (3) (1998) 1655.
[5] J. Roth, J. Nucl. Mater. 266–269 (1999) 51.
[6] G. Federici et al., J. Nucl. Mater. 266–269 (1999) 14.
[7] J. Roth, J. Bohdansky, J.B. Roberto, J. Nucl. Mater. 128&129 (1984) 534.
[8] Y. Hirooka et al., J. Nucl. Mater. 176–177 (1990) 473.
[9] T. Hino, T. Yamashina, S. Fukuda, Y. Takasugi, J. Nucl. Mater. 186 (1991) 54.
[10] C. García-Rosales, E. Gauthier, J. Roth, R. Schwörer, W. Eckstein, J. Nucl. Mater. 189 (1992) 1.
[11] J. Roth, C. García-Rosales, R. Behrisch, W. Eckstein, J. Nucl. Mater. 191–194 (1992) 45.
[12] J.W. Davis, A.A. Haasz, J. Nucl. Mater. 195 (1992) 166.
[13] C. García-Rosales, J. Roth, J. Nucl. Mater. 196–198 (1992) 573.
[14] T. Hino, K. Ishio, Y. Hirohata, T. Yamashina, T. Sogabe, M. Okada, K. Kuroda, J. Nucl. Mater. 211 (1994) 30.
[15] C. García-Rosales, J. Roth, R. Behrisch, J. Nucl. Mater. 212–215 (1994) 1211.
[16] Y.K. Allen, A.A. Chen, Haasz, J.W. Davis, J. Nucl. Mater. 227 (1995) 66.
[17] J. Roth, H. Plank, R. Schwörer, Phys. Scr. T64 (1996) 67.
[18] A. Pospieszczyk, V. Philipps, E. Casarotto, U. Kogler, B. Schweer, B. Unterberg, F. Weschenfelder, J. Nucl. Mater. 241–243 (1997) 833.
[19] J.W. Davis, A.A. Haasz, J. Nucl. Mater. 255 (1998) 214.
[20] C.H. Wu, C. Alessandrini, P. Bonal, H. Grote, R. Moormann, M. Roedig, J. Roth, H. Werle, G. Vieider, J. Nucl. Mater. 258–263 (1998) 833.
[21] J.P. Qian, J. Roth, J.R. Song, F. Zhang, L. Yang, G.T. Zhai, J. Nucl. Mater. 258–263 (1998) 706.
[22] M. Balden, Phys. Scr. T81 (1999) 64.
[23] R. Jimbou, K. Nakamura, V. Bandourko, M. Dairaku, Y. Okumura, M. Akiba, J. Nucl. Mater. 266–269 (1999) 1103.
[24] P. Franzen, E. Vietzke, J. Vac. Sci. Technol. A 12 (1994) 820.
[25] A.A. Haasz, J.W. Davis, J. Nucl. Mater. 232 (1996) 219.
[26] M. Mayer, M. Balden, R. Behrisch, J. Nucl. Mater. 252 (1998) 55.
[27] M. Rubel, N. Almqvist, P. Wienhold, C.h. Wu, J. Nucl. Mater. 258–263 (1998) 787.
[28] H. Marsch, A.P. Warburton, Carbon 14 (1976) 47.
[29] A. Ōya, H. Marsh, J. Mater. Sci. 17 (1982) 309.
[30] V.N. Parmon, Catal. Today 51 (1999) 435.
[31] C.E. Lowell, J. Am. Ceram. Soc. 50 (1967) 142.
[32] S. Marinković, in: P.A. Thrower (Ed.), Chemistry and Physics of Carbon, vol. 19, Marcel Dekker, New York, 1984, p. 1.
[33] A. Horn, A. Schenk, J. Biener, B. Winter, C. Lutterloh, M. Wittmann, J. Küppers, Chem. Phys. Lett. 231 (1994) 193.
[34] M. Wittmann, J. Küppers, J. Nucl. Mater. 227 (1996) 186.
[35] H. Grote, W. Bohmeyer, H.-D. Reiner, T. Fuchs, P. Kornejew, J. Steinbrink, J. Nucl. Mater. 241–243 (1997) 1152.
[36] H. Grote, W. Bohmeyer, P. Kornejew, H.-D. Reiner, G. Fussmann, R. Schlögl, G. Weinberg, C.H. Wu, J. Nucl. Mater. 266–269 (1999) 1059.
[37] A. Schenk, B. Winter, C. Lutterloh, J. Biener, U.A. Schubert, J. Küppers, J. Nucl. Mater. 220–222 (1995) 767.
[38] R. Schwörer, J. Roth, J. Appl. Phys. 77 (1995) 3812.
[39] H. Plank, R. Schwörer, J. Roth, Surf. Coat. Technol. 83 (1996) 93.
[40] M. Balden, J. Roth, J. Nucl. Mater. 279 (2000) 351.
[41] M. Balden, S. Picarle, J. Roth, these Proceedings.
[42] G. Betz, G.K. Wehner, in: R. Behrisch (Ed.), Sputtering by Particle Bombardment II, vol. 52, Springer, Berlin, 1983, p. 18.
[43] M. Balden, C. García-Rosales, R. Behrisch, J. Roth, P. Paz, J. Etxeberria, these Proceedings.
[44] P. Paz, C. García-Rosales, J. Etxeberria, M. Balden, J. Roth, R. Behrisch, Development of Doped Graphite for Plasma-facing Components, presented at the 21st SOFT, 11–15 September 2000, Madrid, Spain.
[45] K. Hüttinger, Adv. Mater. 2 (8) (1990) 349.
[46] M. Braun, A. Gschwindt, W.R. Hoffmann, K. Hüttinger, Ber. DKG 72 (10) (1995) 631.
[47] B. Sundman, B. Jansson, J.O. Andersson, The Thermo-Calc Databank System, Calphad 2 (153) (1985).
[48] R.J. Kotelinikof et al., Handbook on Super Refractory Materials, Metallurgy publisher, Moscow, 1976.
[49] W. Delle, K. Koizlik, H. Nickel, Graphitische Werkstoffe für den Einsatz in Kernreaktoren, Teil 2: Polykristalliner Graphit und Brennelementmatrix, Karl Thiemig Ag, Munich, 1983, p. 40.
[50] T.A. Burtseva, O.K. Chugunov, E.F. Dovguchits et al., J. Nucl. Mater. 191–194 (1992) 309.
[51] R. Behrisch, J. Venus, J. Nucl. Mater. 202 (1993) 1.
[52] V.N. Lipatnikov, A.I. Gusev, P. Ettmayer, W. Lengauer, J. Phys.: Condens. Matter 11 (1999) 163.
[53] W. Eckstein, C. García-Rosales, J. Roth, W. Ottenberger, Sputtering Data, Technical Report IPP 9/82, Max-Planck-Institut für Plasmaphysik, Garching, 1993.